Corrosion of Ag-Ag_2O in Iodide Solutions: A Potential Radioiodine Immobilization Route

S. Pretty, P.Keech, X. Zhang, and J.C. Wren[1]
[1] University of Western Ontario, Ontario, Canada

Abstract

The reaction kinetics of Ag_2O films on Ag with aqueous iodide forming AgI were followed by a novel method of monitoring open-circuit potential (E_{OC}) under static and rotating conditions. The solid-liquid interfacial kinetic parameters can then be determined by measuring τ_f as a function of surface area of Ag_2O and I^- concentration. In this study, the application of the technique is extended to examine the effect of mass transport on the reaction kinetics by measuring τ_f as a function of electrode rotation rate.

1. Introduction

One safety concern for nuclear power reactors is the potential for the public to be exposed to a radiation dose in the unlikely event of a severe nuclear accident. In such an accident scenario, a primary concern is the reactor inventory of fission product radioiodine, due to its radiological toxicity and potential for release to outside atmosphere [1–10]. It is postulated that radioiodine would be released from the fuel, into the fuel channel and subsequently into the containment building, and that although initially released into the containment as airborne species (aerosols and vapors), it would quickly dissolve as non-volatile iodide in water ubiquitously present throughout the building. A small fraction may, however, remain airborne, or revolatilize and become airborne again via the continuous conversion of non-volatile I^- to volatile I_2 or organic iodides in water by ionizing radiation. For the analysis of the consequence of such an accident and post-accident management, it is important to assess the airborne fraction of radioiodine over a long period until the radioactivity of iodine decreases to a safe level [1–10].

One of the reactions that may control iodine volatility under the post-accident containment conditions is its reaction with silver. Nuclear reactors have built-in special safety systems for potential upset events, including shutdown systems to absorb neutrons and stop the chain reactions. The most common shutdown system is solid mechanical shutdown rods, typically made of silver-cadmium, where cadmium is the neutron absorber and silver is added for structural support. In a severe accident scenario, it is postulated that control rods would melt and release silver from the reactor core into the containment building. Accordingly, severe-accident simulation experiments [13,14] have shown a significant release of Ag into the containment vessel, consequently leading to a more significant reduction in iodine volatility than initially predicted, and attributed this to the silver iodine interactions forming highly insoluble and non-volatile silver iodide.

Under the postulated severe accident conditions, silver may enter the aqueous phase as a variety of species (Ag, AgOH, Ag_2O and AgO), and the reactivities differ widely depending on iodine species. Since the speciation of silver and iodine may evolve with time under the dynamic irradiation conditions, determination of the airborne iodine fraction requires quantitative understanding of the reaction kinetics and mechanisms of individual species of silver and iodine.

We have previously investigated the solid-solid conversion of Ag_2O to AgI on Ag substrate in phosphate-buffered iodide solutions using a novel electrochemical method [11,12]:

$$Ag_2O + 2\ I^- + H_2O \rightarrow 2\ AgI + 2\ OH^- \quad (1)$$

These studies have demonstrated that completion of the conversion of Ag_2O to AgI brings about a sudden drop in open circuit potential, E_{OC}, which allows easy and accurate determination of the total reaction time, τ_f [11]. Kinetic parameters are then easily determined from the total reaction time measured as a function of the initial amount of Ag_2O on Ag and I^- concentration [11].

Our previous studies were performed under stagnant conditions. Since the observed net reaction rate was approaching the aqueous diffusion-controlled rate, there is a strong possibility that the rate might have been mass transport limited. To separate the contribution of I^- transport to the Ag_2O surface from the reaction kinetics at the surface, the Ag_2O to AgI conversion has also been investigated as a function of electrode rotation rate in this study.

2. Experimental Procedure

A three-electrode system, consisting of a silver working electrode (area of 0.385 cm^2), a platinum mesh counter electrode, and a saturated calomel reference electrode (SCE) was used for all electrochemical measurements. All potentials are quoted against the SCE scale (+241 mV *vs.* standard hydrogen electrode). All experiments were conducted at room temperature in either Ar-purged 0.01 mol dm^{-3} NaOH (Caledon, 97.0 % purity) or 0.02 mol dm^{-3} NaH_2PO_4 (Caledon, 97.0 % purity) with the pH adjusted to 12 with NaOH (Celedon, Reagent Grade). All solutions have been prepared with water purified using a NANOpure Diamond UV ultra-pure water system (Barnstead International) with a resistivity of 18.2 MΩ cm. Potassium iodide solutions were prepared with concentrations in the range 4×10^{-5} to 5×10^{-3} mol dm^{-3}.

Prior to each experiment, the Ag electrode was manually polished with 800, 1000, and 1200 grit silicone carbide papers, washed with Millipore water, ultrasonically cleaned in an acetone/methanol mixture, and re-washed with Millipore water. A potential of -1.1 V was applied for 300 s to cathodically clean the Ag electrode from any air-formed oxide. After cathodic cleaning, a Ag_2O film was grown potentiostatically by applying + 0.4 V, until the total oxidation charge reached a desired value, typically in the range of 0.035 – 0.065 C. These conditions were selected to minimize AgO formation, which is expected to commence at + 0.6 V *vs.* SCE [15,16]. The Ag_2O-covered electrode was then transferred to a 0.01 mol dm^{-3} NaOH solution containing a known amount of KI. The reaction between Ag_2O and I^- was monitored by measuring the open circuit potential (E_{OC}) as a function of time.

The morphology of the electrode surface under varying solution conditions were obtained with a Hitachi S-4500 field emission SEM equipped with a Quartz Xone energy dispersive X-ray (EDX) analysis system to analyze the elements present on the surface. Micro X-Ray Diffraction data was conducted on a Bruker™ D8 Discover diffractometer in an off-coupled scan mode where $\theta_1 = 6$, and $\theta_2 = 16.5$ and beam diameter was 300 μm. The diffractometer was operated with Cu$K\ \alpha$ radiation generated at 40 kV and 40 mA.

3. Results & Discussion

The rate of a solid-liquid interaction is determined by both the transport of the aqueous reactant, I^-, to the reactant surface, and the kinetics of the reaction between I^- and Ag_2O on the surface. The overall rate constant, k_{app}, of the binary kinetic system is typically expressed as

$$\frac{1}{k_{app}} = \frac{1}{k_{mass}} + \frac{1}{k_{surf}} \tag{2}$$

where k_{mass} is the mass transport coefficient and k_{surf} is the surface reaction rate constant. The results reported previously were collected under stagnant conditions, and the observed rate constant approached an aqueous diffusion-controlled rate. This indicates that the apparent reaction rate might have been mass transport limited, and to determine whether this was the case, the Ag_2O to AgI conversion kinetics was studied as a function of electrode rotation rate.

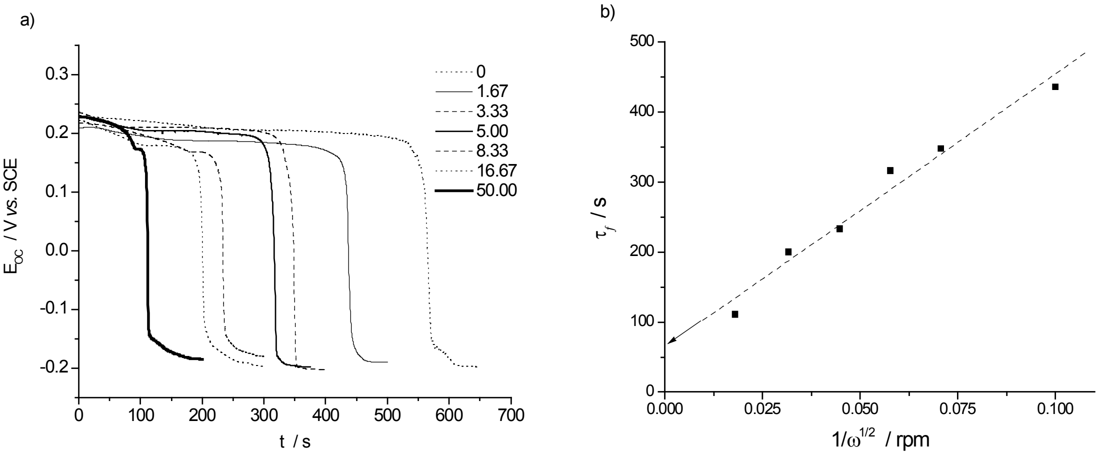

Figure 1: (a) E_{OC} as a function of reaction time and its dependence on rotation speed; b) total reaction time *vs.* $(1/\omega^{1/2})$. The reaction conditions were oxides grown to $(Q_{Ag_2O})_o$ of 0.05 C, $[I^-]_0$ = 5×10^{-4} mol dm^{-3} under phosphate-free solution, and rotation speed ranging from 0 to 50 Hz.

Figure 1a shows the effect of electrode rotation rate on the E_{OC} behaviour. The electrode rotation does not affect the general trend in E_{OC}; it initially remains close to $(E^e)_{Ag_2O/Ag}$, but drops to $(E^e)_{AgI/Ag}$ immediately upon completion of the conversion. The total reaction time determined by the major transition in E_{OC} is a strong function of the rotation rate. The solution to the convective-diffusion equation describing transport at a rotating disk is well established [20] and provides the diffusion boundary layer thickness, δ_{diff}, as a function of electrode angular velocity, ω:

$$\delta_{diff} = 1.61 \cdot D^{1/3} \cdot \omega^{-1/2} \cdot \nu^{1/6} \tag{3}$$

where v is the kinematic viscosity and has units of $\mathrm{cm^2\ s^{-1}}$, and $\omega = 2\pi f$, where f is the rotation frequency. Since the mass transport rate is inversely proportional to δ_{diff},

$$\frac{1}{k_{mass}} \propto \omega^{-1/2} \tag{4}$$

From equation 2, 3, and 4,

$$\tau_f = \tau_{surf} + C_{diff} \cdot \omega^{-1/2} \tag{5}$$

with,

$$\tau_{surf} = \frac{(Q_{Ag_2O})_0}{F \cdot (A_{Elec}) \cdot [I^-]_0} \cdot \frac{1}{k_{surf}} \tag{6}$$

where τ_{surf} is the total reaction time at infinitely fast electrode rotation and C_{diff} is a proportionality constant.

Equation 6 states that τ_f would increase linearly with $\omega^{-1/2}$, and the intercept of the τ_f *vs.* $\omega^{-1/2}$ plot provides a value of τ_{surf} from which the surface reaction rate constant, k_{surf}, can be obtained. The τ_{surf} value obtained using the least-square analysis in phosphate-free NaOH solutions (Figure 1b). It was determined to be 64 s for an initial Ag_2O film grown to a total charge of 0.05 C, and exposed to 5×10^{-4} M I^-, resulting in $k_{\mathrm{surf}} = 4.2 \times 10^{-2}\ \mathrm{cm\ s^{-1}}$. This value is about an order of magnitude larger than the net rate constant obtained under static conditions, indicating that the aqueous transport of I^- to the Ag_2O surface is the rate determining step under stagnant conditions.

To investigate the influence of phosphate in more detail the experiments with rotating electrodes were also conducted with phosphate present during both the growth of the Ag_2O film and the chemical conversion. The results obtained with phosphate present also show the same electrode-rotation dependence of τ_f: an increase in electrode rotation rate results in a decrease in τ_f. The k_{surf} in phosphate solution is determined to be $7.5 \times 10^{-2}\ \mathrm{cm\ s^{-1}}$ (results not shown). This value is ~ 20 times larger than the net rate constant obtained with no rotation in phosphate solution.

The surface reaction rate constant observed in the presence of phosphate is approximately twice that observed in the absence of phosphate: 7.5×10^{-2} *vs.* $4.2 \times 10^{-2}\ \mathrm{cm\ s^{-1}}$. The difference is small, only slightly larger than experimental uncertainty which is estimated to be ~ ± 35 %, and is partially attributed to the difference in the initial surface area $(A_{Ag_2O})_0$ of the Ag_2O films grown in the presence and absence of phosphate.

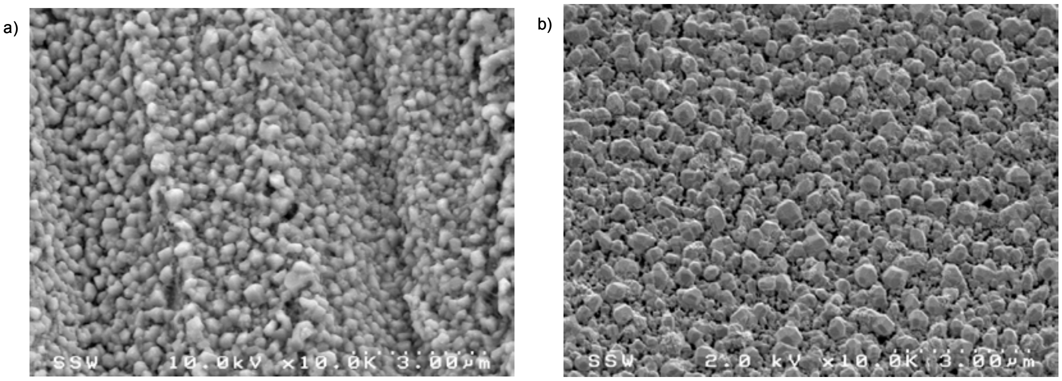

Figure 2: SEM images of a Ag_2O film grown to $(Q_{Ag_2O})_0$ of 0.05 C in the absence of phosphate (a) and in the presence of phosphate (b).

SEM images of Ag_2O films grown with the same amount of charge, 0.05 C in phosphate-free and 0.02 mol dm^{-3} NaH_2PO_4 solutions are compared in Figure 2. The Ag_2O crystals grown in NaH_2PO_4 solution vary in diameter, with a dimension typically in the range of 200 – 500 nm, whereas those grown in phosphate-free solutions are more evenly sized and typically 200 nm in diameter. This difference likely arises from the different rates of film growth in the two solutions; films grown in the presence of phosphate generally grow much faster.

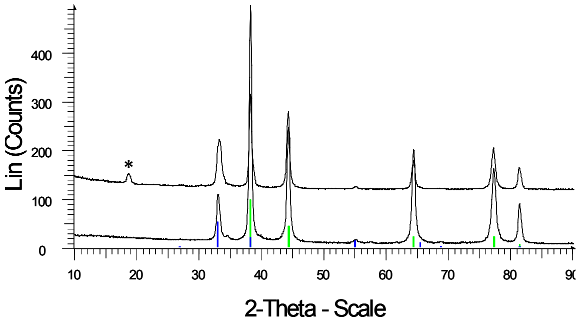

Figure 3: μ-XRD patterns recorded for oxides grown in the presence of 0.02 mol dm^{-3} NaH_2PO_4 (top pattern) and in phosphate-free NaOH (bottom pattern). The experimental conditions were oxides grown to $(Q_{Ag_2O})_o$ of 0.05 C at + 0.4 V. The black diffraction lines correspond to silver, and the grey diffraction lines to correspond to silver oxide. The asterisk identifies the peak not present in the phosphate-free Ag_2O diffraction pattern.

Another possible contributor to the different surface reaction rates is the incorporation of phosphorous into the Ag_2O matrix during initial anodic Ag_2O film growth in phosphate solutions. Surface analysis by XRD support the hypothesis that incorporation of phosphate into the Ag_2O matrix occurs. A clear difference in the X-ray diffraction pattern, Figure 3, is observable as a peak at $2\theta = 18^{o}$ appears in the diffraction pattern of the Ag_2O film grown in phosphate-containing solutions. This peak is absent from the pattern of the Ag_2O film grown in NaOH and does not correspond to NaH_2PO_4, which may precipitate on the surface in the event of insufficient electrode rinsing.

Nevertheless, its presence in the oxide matrix does not seem to have any influence on the mechanism or kinetics of the conversion, as the surface reaction rates in both solutions are very similar. Considering the variability in surface area discussed above, the rates show that neither the incorporation of phosphate into the Ag_2O film, nor its presence during the interaction of Ag_2O with I^-, significantly affects the reaction orders or the rate constant.

4. Conclusions

The reaction kinetics of the Ag_2O film on Ag substrate with aqueous I^- to form AgI was followed by monitoring open-circuit potential. Complete conversion of Ag_2O to AgI was indicated by an abrupt transition in the E_{OC} from a value close to $(E^e)_{Ag_2O/Ag}$ to a value close to $(E^e)_{AgI/Ag}$, allowing for an easy determination of the total reaction time, τ_f. The kinetic parameters of the solid Ag_2O and aqueous iodide reaction were then determined by measuring τ_f as a function of the amount of Ag_2O anodically formed on Ag and the aqueous concentration of I^-.

The effect of mass transfer on the reaction kinetics was investigated by measuring the total reaction time as a function of electrode rotation rate. The total reaction time was found to be inversely proportional to the square root of the rotation rate, and extrapolation of the rotation rate dependence to infinite rotation speed enabled us to determine a surface chemical reaction rate with reasonable accuracy. This surface reaction rate constant was about an order of magnitude larger than the net conversion rate constant obtained under stagnant conditions, indicating that the conversion is largely mass-transfer limited under stagnant conditions.

The influence of phosphate in electrolytes on the conversion reaction was also investigated. The surface reaction rate constant in phosphate solutions was approximately twice that in the absence of phosphate: 7.5×10^{-2} *vs.* 4.2×10^{-2} cm s^{-1}. This difference is small, and is partially attributed to the difference in the initial surface area or surface structure $(A_{Ag_2O})_0$ of the Ag_2O films grown in the presence and absence of phosphate. Although the XRD analysis results suggest the incorporation of phosphorous into the Ag_2O matrix during the initial anodic Ag_2O film growth in phosphate solutions, this study suggests that its presence does not seem to have any influence on the mechanism or kinetics of the conversion.

5. References

[1] J. McFarlane, J.C. Wren, R.J. Lemire, J. Nucl. Tech. 138 (2002) 162.
[2] J.C. Wren, J.M. Ball, Rad. Phys. Chem. 60 (2001) 577.
[3] J.C. Wren, J.M. Ball, G.A. Glowa, J. Nucl. Tech. 129 (2000) 297.
[4] J.C. Wren, Proc. European Rev. Meet. Severe Acc. Research (ERMSAR-2005), Aix-en-Provence, France, 14-16 November 2005.
[5] F. Taghipour, G.J. Evans, Nucl. Tech. 137 (2002) 181.
[6] S. Güntay, R.C. Cripps, B. Jäckel, H. Bruchertseifer, Nucl. Tech. 150 (2005) 303.
[7] L. Cantrel, P. March, Nucl. Tech. 154 (2006) 170.
[8] Q.W. Parker, C.J. Barton, Fission Product Release, The Technology of Nuclear Reactor Safety, Vol. 2, The M.I.T. Press, Cambridge, MA, 1973.

[9] F. Garisto, R.J. Lemire, J. Paquette, P.P.S. Saluja, S. Sunder, D.F. Torgerson, A.C. Vikis, D.J. Wren, J.C. Wren, Proc. Series of an Internat. Sympo. On Source Term Evaluation for Accident Conditions, Columbus, OH, 1986, p. 501.
[10] L.Soffer, S.B. Burson, C.M. Ferrell, R.Y. Leem J.N. Ridgely, Accident Source Terms for Light-Water Nuclear Power Plants, Washington, DC, NUREG-1465GAR, Vol. 95, Issue 13, 1995.
[11] X. Zhang, S.D. Stewart, D.W. Shoesmith, J.C. Wren, J. Electrochem. Soc. 154 (2007) F70.
[12] X. Zhang, D.W. Shoesmith, J.C. Wren, Corr. Sci. 50 (2008) 490.
[13] D. Jacquemain, N. Hanniet, C. Poletiko, S. Dickenson, C. Wren, D.A. Powers, E. Krausmann, F. Funke, R. Cripps, B. Herrero, Proc. of the OECD Workshop on Iodine Aspects of Severe Accident Management, Vantaa, Finland, 1999, p.57.
[14] N. Girault, S. Dickenson, F. Funke, A. Auvinen, L. Herranz, E. Krausmann, Nucl. Eng. Des., 236 (2006) 1293.
[15] J. Kunze, H.H. Strehblow, G. Staikov, Electrochem. Commun., 6 (2004) 132.

[16] D. Lützenkirchen-Hecht, H-H. Strehblow, Surf. Interface Anal., 38 (2006) 686.
[17] E. Krausmann, Y. Drossinos, J. Nucl. Mat., 264 (1999) 113.
[18] G. Cohn, Chem. Rev., 42 (1948) 527.
[19] M. Fleischmann, K. Korinek, D. Pletcher, J. Chem. Soc., Perkin Trans. 2, (1972) 1396.
[20] A.J. Bard, L.R. Faulkner, Electrochemical Methods: Fundamentals and Applications, 2nd ed., John Wiley & Sons Inc., Hoboken, NJ, 2001, pp 337-339.